

ARTICLE

An Overview of Oligocene to Recent Sediments of the Western Pacific Warm Pool (WPWP) (International Ocean Discovery Program-IODP Exp. 363) Using Warm and Cool Foraminiferal Species

Patrícia Pinheiro Beck Eichler^{1,2*} Christofer Paul Barker² Moab Praxedes Gomes¹
Helenice Vital¹

1. Programa de Pós-Graduação em Geodinâmica e Geofísica (PPGG), Universidade Federal do Rio Grande do Norte (UFRN), Campus Universitário, Lagoa Nova, 59072-970 - Natal, RN, Brazil

2. Ecologic Project, Boulder Creek, California, United States

ARTICLE INFO

Article history

Received: 4 August 2021

Accepted: 12 August 2021

Published Online: 13 August 2021

Keywords:

Miocene

Population dynamics

Climate change

Tolerance

Temporal

Spatial

ABSTRACT

We use the excellent sediment recovery of International Ocean Discovery Program (IODP) Exp. 363, in the Western Pacific Warm Pool (WPWP) to assess down-core variations in the abundance of warm versus cool benthic foraminiferal species through a warm benthic foraminifera (WBF) curve. The total percentage of the “warm” shallower species group (*Laticarinina pauperata*, *Cibicides kullenbergi*, *C. robertsonianus*, *Cibicides sp.*, *Hoeglundina elegans*, and *Bulimina aculeata*) and of the “cool” species group from deep waters (*Pyrgo murrhina*, *Planulina wuellerstorfi*, *Uvigerina peregrina*, and *Globobulimina hoeglundi*, *Hopkinsina pacifica*) at all sites is used to assess paleo temporal and spatial variations in preservation and marine temperature. Our study sites span water depths ranging from 875 m to 3421 m and our results indicate that well-preserved living and fossil foraminifera characterize mudline and core sediments at all water depths attesting the wide environmental tolerance of these species to temperature and pressure. Using magneto-and biostratigraphy datum, these sediments are of Oligocene age. Our low-resolution study showed that with the exception of core 1486B which the linear tendency of warmer species is toward cool sediments in old times, all of them show that older sediments indicate warmer periods than today, which is expected from Miocene to Recent. Our results provide evidence for the preservation potential of deeply buried sediments, which has implications on climate reconstructions based on the population dynamics of calcareous benthic foraminifera.

1. Introduction

Benthic foraminifera have been used to reconstruct environmental conditions in all marine and transitional environments, from hypersaline lagoons^[1] and coral

reefs^[2-4] along the coast to deep sea^[5]. Relative abundances of foraminiferal species and assemblages have been calibrating recent environmental characteristics of marine environments in mangrove and estuaries^[6-9] and

*Corresponding Author:

Patrícia Pinheiro Beck Eichler;

Programa de Pós-Graduação em Geodinâmica e Geofísica (PPGG), Universidade Federal do Rio Grande do Norte (UFRN), Campus Universitário, Lagoa Nova, 59072-970 - Natal, RN, Brazil; Ecologic Project, Boulder Creek, California, United States;

Email: patriciaeichler@gmail.com

in upwelling in continental shelves^[10,11]. In the Atlantic restricted environments of Delaware inland Bays, USA,^[8] traced East-West gradient salinity using *Ammonia* and *Elphidium* species, and have resolved both temperature and salinity variations in Rehoboth Bay. These recent studies show balance of thermohaline features and productivity of shelf-water masses using the stable isotopic composition of benthic foraminiferal. Three major assemblages of benthic foraminiferal from slopes of Ashmore Trough (Gulf of Papua) provided information about the paleo environmental history of modern tropical mixed siliciclastic-carbonate system, in the last ~83 kyr, which, is likely to be linked to sea level-driven changes in the amount of siliciclastic, carbonate, organic matter, and bottom water oxygen concentrations^[12].

Here we deal with faunal fluctuations related to cool or warm phases, in the same faunal groups proposed by Lutze in 1977. In these studies^[13,14] uses total percentages proportion of “warm” benthic species (*Laticarinina pauperata*, *Cibicidoides kullenbergi*, *C. robertsonianus*, *Cibicidoides* sp., *Hoeglundina elegans*, and *Bulimina aculeata*) and of “cool” species group (*Pyrgo murrhina*, *Planulina wuellerstorfi*, *Uvigerina peregrina*, *Globobulimina hoeglundi*, and *H. pacifica*) while percentages of all other species were ignored, resulting in the warm benthic foraminifera (WBF) curve”. Relative abundance of above mentioned warm species and

cool species collected in the Expedition 363 sites in the Western Pacific Warm Pool (WPWP) from the continental slope of northwestern Australia and of Papua New Guinea by the International Ocean Discovery Program (IODP) provides insights on the WBF curve and preservation state. These data track reconstruction of temporal and spatial variations from late Oligocene (~24 mya) to Recent in water depths ranging from 875 to 3421 m, and in sediment columns (at least up to 550 m) allowing convenient comparison. Our data reflect past interglacial and glacial cycles in the last 23 Myr tracking paleoclimate variations with well preserved material.

2. Study Area

We investigated the mudlines and cores of nine sites drilled during Exp. 363 (Figure 1, Table 1).

Two of the sites U1482A (Lat. 15°03.3227'S, Long. 120°26.1049'E) and U1483A (Lat. 13°05.2382'S, Long. 121°48.2424'E) are located at 1467.70 and 1732.93 m water depth off northwestern Australia at the southern part of the WPWP. Four sites lie in the Manus basin on the northern border of Papua New Guinea: U1484A at 1030.93 m water depth (Lat. 03°07.9228'S, Long. 142°46.9699'E); U1485A at 1144.75 m (Lat. 03°06.1585'S, Long. 142°47.5750'E); U1486B at 1333.83 m (Lat. 02°22.3368'S, Long. 144°36.0794'E), and U1487A at 873.93 m (Lat. 02°19.9979'S, Long. 144°49.1627'E). Three further sites

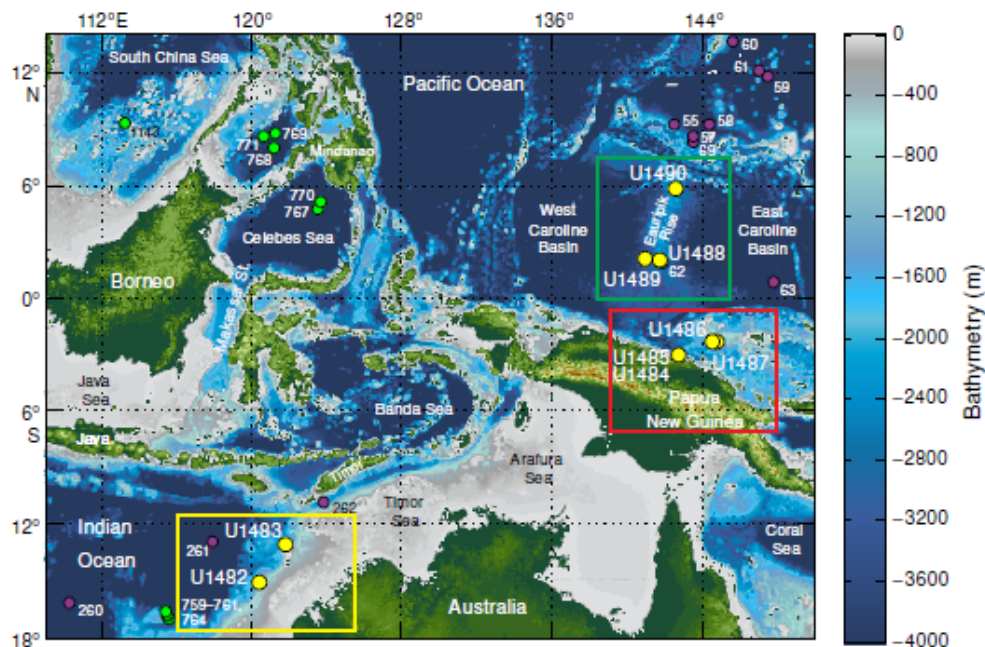


Figure 1. Bathymetric map with three areas cored in the IODP WPWP Exp. 363: Northwestern Australian shelf, Papua New Guinea/Manus Basin, Eauripik Rise.

Yellow circles = Expedition 363 sites, purple and green circles = earlier on cored DSDP and ODP sites. Source and analysis from Amante and Eakins (2009).

Table 1. Expedition 363 Hole summary DSF=drilling depth below seafloor.

Hole	Latitude	Longitude	Water depth (m)	Penetration (m DSF)	Cored interval (m)	Recovered length (m)	Recovery (%)	Drilled interval (m)	Drilled interval (N)	Total cores (N)	APC cores (N)	HLAPC cores (N)	XCB cores (N)	Date started (2016)	Time started (h UTC)	Date finished (2016)	Time finished (h UTC)	Time on hole (days)
U1482A	15°3.3227'S	120°26.1049'E	1467.70	490.0	490.0	505.88	103.24	0.0	0	58	37	8	13	16 Oct	0730	19 Oct	0810	3.03
U1482B	15°3.3142'S	120°26.0988'E	1464.49	366.6	349.1	365.82	104.79	17.5	5	40	35	5	0	19 Oct	0810	20 Oct	1600	1.33
U1482C	15°3.3298'S	120°26.1135'E	1465.19	534.1	517.1	535.86	103.63	17.0	4	56	34	0	22	20 Oct	1600	24 Oct	1500	3.96
U1482D	15°3.3305'S	120°26.0920'E	1466.13	213.0	80.4	82.77	102.95	132.6	1	9	9	0	0	24 Oct	1500	25 Oct	1000	0.79
U1483A	13°05.2382'S	121°48.2424'E	1732.93	293.3	293.3	308.58	105.21	0.0	0	31	31	0	0	25 Oct	2230	27 Oct	1650	1.76
U1483B	13°05.2371'S	121°48.2538'E	1734.01	287.0	287.0	301.62	105.09	0.0	0	31	31	0	0	27 Oct	1650	28 Oct	1810	1.06
U1483C	13°05.2479'S	121°48.2537'E	1731.19	284.8	281.8	292.42	103.77	3.0	1	30	30	0	0	28 Oct	1810	30 Oct	0000	1.24
U1484A	03°07.9228'S	142°46.9699'E	1030.93	223.2	223.2	220.60	98.84	0.0	0	27	21	6	0	6 Nov	1245	7 Nov	1755	1.22
U1484B	03°07.9223'S	142°46.9809'E	1030.48	222.9	220.9	220.51	99.82	2.0	1	30	17	13	0	7 Nov	1755	8 Nov	2250	1.2
U1484C	03°07.9335'S	142°46.9822'E	1030.77	221.4	219.4	225.46	102.76	2.0	1	31	17	14	0	8 Nov	2250	9 Nov	2345	1.04
U1485A	03°06.1585'S	142°47.5750'E	1144.75	300.8	300.8	312.36	103.84	0.0	0	44	20	24	0	9 Nov	2345	11 Nov	1210	1.52
U1485B	03°06.1584'S	142°47.5854'E	1145.34	297.7	295.7	291.18	98.47	2.0	1	46	20	26	0	11 Nov	1210	12 Nov	2125	1.39
U1485C	03°06.1574'S	142°47.5991'E	1145.83	27.5	27.5	29.35	106.73	0.0	0	3	3	0	0	12 Nov	2125	13 Nov	0255	0.23
U1485D	03°06.1574'S	142°47.5867'E	1144.43	63.9	62.9	68.22	108.46	1.0	1	7	7	0	0	13 Nov	0255	13 Nov	1330	0.44
U1486A	02°22.3375'S	144°36.0796'E	1330.33	9.5	9.5	9.95	104.74	0.0	0	1	1	0	0	13 Nov	2321	14 Nov	0600	0.28
U1486B	02°22.3368'S	144°36.0794'E	1333.83	211.2	211.2	215.49	102.03	0.0	0	23	23	0	0	14 Nov	0600	15 Nov	0250	0.87
U1486C	02°22.3478'S	144°36.0798'E	1334.50	201.3	197.3	172.70	87.53	4.0	2	21	21	0	0	15 Nov	0250	16 Nov	0010	0.89
U1486D	02°22.3484'S	144°36.0690'E	1334.10	186.5	162.7	166.53	102.35	23.8	1	18	16	0	0	16 Nov	0010	17 Nov	0018	1.01
U1487A	02°19.9979'S	144°49.1627'E	873.93	144.2	144.2	146.43	101.55	0.0	0	16	16	0	0	17 Nov	0145	17 Nov	2040	0.79
U1487B	02°19.9975'S	144°49.1746'E	873.63	144.3	144.3	148.73	103.07	0.0	0	18	14	4	0	17 Nov	2040	18 Nov	1215	0.65
U1488A	02°02.5891'S	141°45.2864'E	2603.40	314.5	314.5	327.20	104.04	0.0	0	35	32	3	0	19 Nov	1800	21 Nov	1520	1.89
U1488B	02°02.5901'S	141°45.2966'E	2604.40	304.9	304.9	315.77	103.57	0.0	0	33	33	0	0	21 Nov	1520	23 Nov	0140	1.43
U1488C	02°02.5793'S	141°45.2974'E	2604.00	159.3	159.3	153.60	96.42	0.0	0	17	17	0	0	23 Nov	0140	24 Nov	0030	0.95
U1489A	02°07.1976'S	141°01.6654'E	3419.80	9.5	9.5	9.53	100.32	0.0	0	1	1	0	0	24 Nov	0442	24 Nov	1515	0.44
U1489B	02°07.1984'S	141°01.6757'E	3419.50	129.2	129.2	120.66	93.39	0.0	0	14	14	0	0	24 Nov	1515	25 Nov	1355	0.94
U1489C	02°07.1772'S	141°01.6746'E	3423.68	385.6	385.6	376.35	97.60	0.0	0	42	29	2	11	25 Nov	1355	27 Nov	1900	2.21
U1489D	02°07.1761'S	141°01.6651'E	3421.55	385.6	238.8	229.24	96.00	146.8	1	26	14	0	12	27 Nov	1900	29 Nov	1612	1.88
U1490A	05°48.9492'S	142°39.2599'E	2341.03	382.8	382.8	367.35	95.96	0.0	0	44	27	4	13	30 Nov	1400	2 Dec	1655	2.12
U1490B	05°48.9507'S	142°39.2698'E	2339.72	262.9	258.9	267.60	103.36	4.0	2	31	24	7	0	2 Dec	1655	4 Dec	0040	1.32
U1490C	05°48.9385'S	142°39.2690'E	2341.27	170.0	164.0	168.24	102.59	6.0	2	18	18	0	0	4 Dec	0040	5 Dec	1942	1.79
Totals:			7227.5	6865.8	6956.00			361.7	23	801	614	116	71					

APC= advanced piston corer, HLAPC = half-length APC, XCB=extended core barrel

lie on the Eauripik Rise in the heart of the WPWP U1488A at 2603.40 m (Lat. 02°02.5891'S, Long. 144°45.2864'E), U1489B at 3419.80 m (Lat. 02°07.1976'S, Long. 141°01.6654'E), and U1490A at 2341.03 m water depth (Lat. 05°48.9492'S, Long. 142°39.2599'E).

Together these sites span a wide spatial and bathymetric range that will allow us to compare sediment cores in the largest source of water vapor to the atmosphere, the Western Pacific Warm Pool (WPWP). Variations in the strength of convection in the WPWP, therefore alter heat and moisture delivery to extra-tropical regions and may amplify changes in global climate^[15,16]. Today WPWP hydrological cycle variability is dominated by (1) the seasonal relocation of the Intertropical Convergence Zone (ITCZ) and subsequent interactions related to the Asian-Australian monsoon and (2) the El Niño Southern Oscillation^[17]. The sedimentary sequences of these sites capture the past 23 Myr at varying burial depths due to differing sedimentation rates allowing us to compare spatial and temporal environmental changes and potential effects of diagenesis on foraminiferal test preservation.

3. Methods

3.1 Sediment Processing

Mudline and core catcher samples from the nine study sites were examined for benthic foraminiferal assemblages. Samples from mudline were sampled by unloading the matter from the top of each core into a bucket, washed

with water through a 63-µm wire mesh sieve. One gram of Rose Bengal diluted in one liter of alcohol was applied to stain living organisms in the mudline samples.

From each core, a catcher of 20-30 cm³ of sediment was washed with water over a 63-µm wire mesh sieve and were looked at for the presence of organisms. Consolidated sediments were immersed in a 3% hydrogen peroxide (H₂O₂) solution, with little amount of Borax, prior to washing, to aid disaggregate hard material. Samples were dried in filter paper in low-temperature oven at ~50°C, and picked up with a fine brush under a binocular stereomicroscope. To prevent mixing of organisms between samples, sieve was cleaned, set into a sonicator for 15 minutes, and inspected for organisms. Species picking and identification were made on the >150 µm size fractions.

3.2 Foraminiferal Counts

Total benthic foraminiferal assemblage composition was built on counts of around 100 specimens. The distribution of lower bathyal and upper abyssal species is set apart into two different groups. Foraminifera belonging to the high carbon flux (>3.5 g C m⁻² year⁻¹), 'warm' (>3.5°C) group are *Bolivina robusta*, *Hoeglundina elegans*, *Globobulimina pacifica*, *Laticarinina pauperata*, *Bulimina aculeate*, and *Cibicidoides pachyderma*; and the lower carbon flux, 'cold' group includes *Oridorsalis umbonatus*, *Uvigerina bifurcata*, and *Planulina wuellerstorfi*^[18]. We counted the relative abundance of "warm" water species and "cool" water species and

calculated the warm benthic foraminifers (WBF) curve. All abundances of other species was counted but is not part of the interpretations.

Figure 2 (a -j) shows preservation status of benthic foraminifera was assessed and classified as: VG = Very Good (zero evidence of abrasion, dissolution, overgrowth); G = Good (low evidence of abrasion, dissolution, or overgrowth); M = Moderate (abrasion, dissolution, overgrowth were common but insignificant); P = poor (considerable abrasion, dissolution, overgrowth, and many fragments).

The illustration shows representative SEM images of the different preservation states at the nine sites. The colors on the back panel of the foraminiferal species (left panel, A) are to visually assign them to different down-core settings (right panel, B). Pictures were taken from the following samples a.1 HCC (0-2mbsf) U1483A; b. 12HCC (100-104mbsf) U1490A; c. 13HCC (104-108 mbsf) U1482A; d. 22HCC (191-195 mbsf) U1490A; e. 43XCC (379-380.1119 mbsf) U1490A; f. 1 HCC (0-2mbsf) U1482A; g. 1HCC (0-2mbsf) U1482A; h. 22HCC (198-202 mbsf) U1486B; i. 35HCC (310 -314.5) U1488A; and j 22HCC (198-202 mbsf) U1490A.

4. Results

4.1 Sedimentological Setting and Microfossil Preservation

U1482A

The core measures ~535 m going to upper Miocene to Pleistocene, rates of sedimentation averaging 5.9 cm/kyr in

the upper Miocene, lessening to ~3.3 cm/kyr in the lower Pliocene. Pleistocene has more elevated sediment rates of ~7.0 cm/kyr [19]. The sediment of this site is composed of nanofossil ooze and chalk with assorted amounts of foraminiferal bathyal forms in a clayed environment. Calcareous species (*Pyrgo* spp., *Laevidentalina* spp., *Uvigerina* spp., *Planulina wuellerstorfi*, and *Hoeglundina elegans*) dominates with lower number of agglutinated forms, the latter representing <5% of the benthic foraminifer assemblages. Diversity ranges from 10 to 26 among studied samples. Sample 26H-CC (240.92 mbsf) shows the highest species diversity and the lowest diversity is from Sample 57X-CC (515.88 mbsf). Paleo depth established from the benthic foraminifer genera and species found in this core, rate as a bathyal bathymetric zone [20]. Shells are very well preserved and rare evidence of mineral overgrowth, abraded tests, and recrystallization was noted (Figure 2a).

U1483A

The sedimentation rate at this site is ~9.0 cm/kyr [21] almost double the rate of Site U1482A, and its location is ~264 km northeast of Site U1482A. This site is composed of nanofossil ooze with different quantities of foraminifers, clay, and diatoms and radiolarians. Calcareous species with lower numbers of agglutinated species (<5% of the assemblages) dominate the assemblages. The most dominant genera and species are *Hoeglundina elegans*, *Pyrgo* spp., *Uvigerina* spp.,

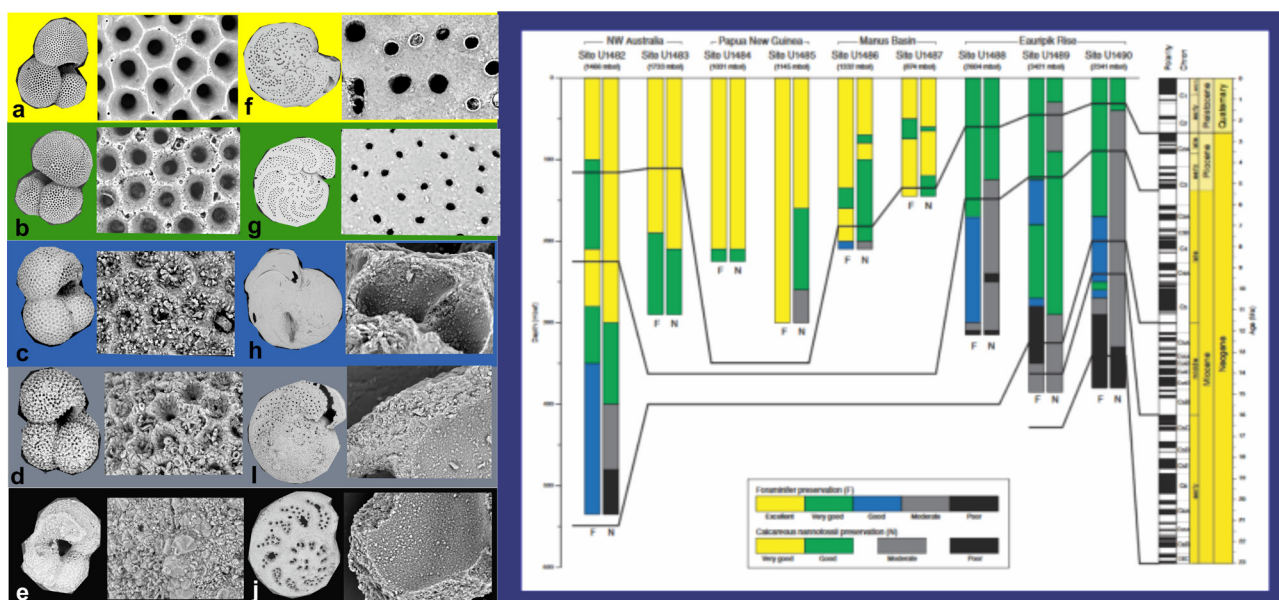


Figure 2 (a - j). Foraminiferal preservation as a function of sediment depth based on visual inspection of planktonic (*Globigerinoides ruber*) and benthic (*Planulina wuellerstorfi*) foraminiferal and nanofossil species (not illustrated) (modified figure from Exp.363 Preliminary report).

Laevidentalina spp., *Planulina wuellerstorfi*. Diversity ranges from 10 to 26 within samples. Sample 10H-CC (94.60 mbsf) shows the highest species diversity and the lowest diversity found in Sample 20H-CC (189.57 mbsf). Paleo depth estimates a bathyal bathymetric zone with shells very well preserved with scarce or with no evidence of abraded shells (Figure 2b).

U1484A

The core presents ~224 m of middle Pleistocene to Recent terrigenous, hemipelagic sediment, containing well-preserved nannofossils, benthic and planktonic foraminifers and it differs from the two previous sites (U1482A and U1483A) because instead of having a deep benthic foraminifera fauna we can see habitats transition in down core catchers samples. This site also differs from previous sites due to the increased abundance and diversity of benthic foraminifera. Benthic foraminifers between Samples U1484A-7H-CC and 17H-CC (62.27-156.48 mbsf) are more dominant than other parts of the hole, and the ratio between benthic foraminifer to planktonic reaches 70:30. Alterations in benthic assemblages are observed downhole, which deeper water benthic foraminifers dominate upper and lower parts of the core; and shallow water benthic foraminifers including reef-dwelling taxa mixed up with deep, dominate the middle section. Alterations in the constitution of the assemblages are described in detail below. Samples U1484A-1H-CC to 6H-CC (5.00-52.95 mbsf) and 17H-CC to 27F-CC (156.48-223.62 mbsf) are mainly constitute of deep-water species: *Cibicidoides pachyderma*, *Bolivina robusta*, *Uvigerina prosboidea*, *U. hispida*, *Bolivinita quadrilateral*, identified as bathyal forms, from depths down to 3500 m^[20,22]. Samples 7H-CC to 9H-CC (62.27-81.21 mbsf) and 15H-CC to 17H-CC (138.62-156.48), are constituted of deep-water species mixed up with the shallow water species *Rotalinoides compressiusculus*, from water depths of 4-70 m^[22]. Reef-dwelling benthic foraminifers as *Operculina complanata* and rare specimens of *Amphisorus hemprichii*, *Coscinospira arietina*, and *Peneroplis planatus* are noted between Samples 10H-CC and 15H-CC (90.58-138.62 mbsf). These species, which are mostly found at water depths <45 m^[22] were probably carried to this specific site with other debris. This transition will be detailed below. The assemblage changed downhole, with deeper water taxa dominating in the upper and lower parts of the sediment core, while middle sections present deep and shallow-water benthic foraminifers mixed with reef-dwelling forms. Preservation is excellent with no calcification or abrasion (Figure 2c).

U1485A

The core length is ~300 m from middle Pleistocene to recent terrigenous and hemipelagic sediment. The upper ~225 mbsf of this site is very similar to Site U1484A, located ~3.2 km distant. Site U1485A contains well-preserved benthic and planktonic foraminifers, and calcareous nannofossils (Figure 2d). Sediment is composed of clay rich foram nanno ooze, sand, and silt. Assemblages are alike to Site U1484A, with less influence from downslope transport. Sandy shallow-water and reef dwelling benthic foraminifers are less frequent at this site comparing to Site U1484A, whereas wood and shells pieces are far more frequent. Hardly any intervals present the shallow-water species *Rotalinoides compressiusculus*, while typical bathyal forms dominate the bulk of the assemblage. Planktonic/benthic foraminifer ratios at this site are around 99:1. Assemblages differ from those at Site U1484A by the presence of deep-water forms without any large contribution from shallower water or reef faunas. A high abundance of volcanic ash in some samples increases the composition of the cool benthic foraminifer assemblage.

U1486B

Sequence of ~211 m of upper Pliocene to recent volcanogenic sediment, authigenic minerals, and biogenic sediment. The sedimentary sequence is signed as late Pliocene linking ages of 2.49 and 3.33 Ma. The sediment core at this site contains benthic and planktonic foraminifers, and nannofossils in extreme excellent preservation, with few foraminifera fragments and cementation or yet incipient recrystallization. Generally, there is no change in the state of shell's preservation with depth (Figure 2e). The assemblage indicates upper bathyal depths all over the core, and ratios around 99:1. It is worthy to mention that the remarkable amount of volcanic ashes a tephra in the sediments below ~130 mbsf most likely influence the diversity and number of foraminifer species.

U1487A

Sequence of ~144 m from upper Pliocene to Recent volcanogenic, biogenic and authigenic sediment, similar to Site U1486B, located 25 km distant. The sedimentary sequence cored shows affinity to Site U1486B. The two sites show the past ~2.7 Myr with reduction in volcanogenic input through time. The sediment core recuperated shows affinity to Site U1486B. The two sites show a decrease in volcanogenic activity through time. A deep-water bathyal environment with a planktonic/benthic

ratio of 99:1, and shell preservation is excellent to very good (Figure 2f) along the core.

Even with sedimentology similarities between the two sites, there are important differences between Site U1487A and Site U1486B, which are lower sedimentation rates, coarser grain size (with different oozes foraminifer versus nannofossil), intensified reworking and bioturbation, with thicker tephra layers and huge fragments.

U1488A

A sequence of ~315 m of upper Miocene to recent, and bio stratigraphic and magnetostratigraphic horizons indicate pelagic sediment from the last ~10 Myr. A foraminifer-rich nannofossil to foraminifer-nannofossil ooze with different proportions of clay in an intermediate to deep bathyal depths^[20,22]. Shell preservation at this site shows recrystallization (foraminifers) and fragmentation, overgrowth (foraminifers and nannofossils) and etching throughout the core (Figure 2g).

U1489B

A sequence of ~386 m of lower Miocene to Recent consists of nannofossil ooze, chalk, and different proportions of clay. Radiolarians are a large composition in the lowermost part of the core. This site show similar increase in recrystallization, fragmentation, etching, and overgrowth seen in site U1488A (Figure 2h).

U1490A

A ~380 m of upper Oligocene to Recent based primarily on downhole variations in biosilica, clay minerals, ashes and tephra. Siliceous microfossils (diatoms, sponge spicules, and radiolarians), calcareous microfossils (nannofossils and foraminifers), clay minerals, and volcanic ashes and tephra dominate this site. Planktonic foraminifers and calcareous nanofossils are present throughout the whole sequence. Benthic foraminifera species show evidence of a deep-water environment, and the planktonic/benthic foraminifer ratio is <99:1 throughout the sequence. The increase in recrystallization (foraminifers), fragmentation, etching, and overgrowth, and the assemblage in general seen downhole are alike to that from Eauripik Rise sites (U1488A and U1489B) (Figure 2h).

4.2. Warm and Cool Benthic Foraminiferal Species

In our low-resolution study of WBF curve it was possible to notice that with the exception of core 1486B, all of them show that older sediments indicate warmer

periods than today, a tendency of what is expected from Miocene to Recent (Figure 3A to 3P, Supplementary Tables 1 to 9 shows abundance of foraminifera species and are available upon request).

Graphs show core catchers samples numbers versus abundance through time.

U1482A

The fauna inversions (cool to warm and vice versa) recorded on Figure 3 shows that upper Miocene (23 to 5.3 Ma) warmer sediments with warm foraminiferal species in rich chalk (Figure 3A) are replaced by cooler foraminifera species in the Pliocene (5.3 to 2.6 Ma) in clay rich nano ooze (Figure 3B). During this time climate became cooler and drier, seasonally similar to modern climate. Towards the end of early Pliocene (3 Ma), a warm foraminifera species rich nano ooze substitute the clay rich nano ooze (with cool foraminifera species) showing fauna inversion. The average temperature in the world during the mid-Pliocene (3.3 Ma-3 Ma) was 2 to 3 °C higher than now and sea level rise of 25 m. In the Northern Hemisphere ice sheet was short-lived before the extensive glaciation over Greenland that took place in the late Pliocene (around 3 Ma) detected by a warm-cool species fauna inversion (Figure 3C). During the early to late Pliocene from 3.6 to 2.2 Ma, the Arctic was warmer than today (with summer temperatures 8 °C warmer than today in the 3.6-3.4 Ma). This is of extreme importance because it is a late Cenozoic marine-based sedimentary record. Later on, in the early to middle Pleistocene (2.5 Ma to 11.7 ka), a nanofossil ooze with cooler foraminifera species is again replaced by warmer species rich nano ooze (Figure 3D).

U1483A

The same fauna inversion in the end of early Pliocene 3.6 to 2.2 Ma when the Arctic was much warmer than today (with summer temperatures 8 °C warmer than today in the 3.6-3.4 Ma, same as U1482A) was recorded on this core (Figure 3A). A fauna inversion on the late Pliocene show the beginning of the extensive glaciation over Greenland that occurred around 3 Ma, and then a clay foram rich nano ooze is changed to diatom foraminifera rich nanno ooze with warmer foraminifera species, same as U1482A (Figure 3B). This epoch is marked by an Arctic ice cap formation noted by a sudden alteration in oxygen isotope ratios and ice-rafted cobbles in the North Atlantic and Pacific Ocean beds, and Mid-latitude glaciation was likely occurring before the end of this Pliocene. The global cooling that happened during the Pliocene may have decreased forests and increase

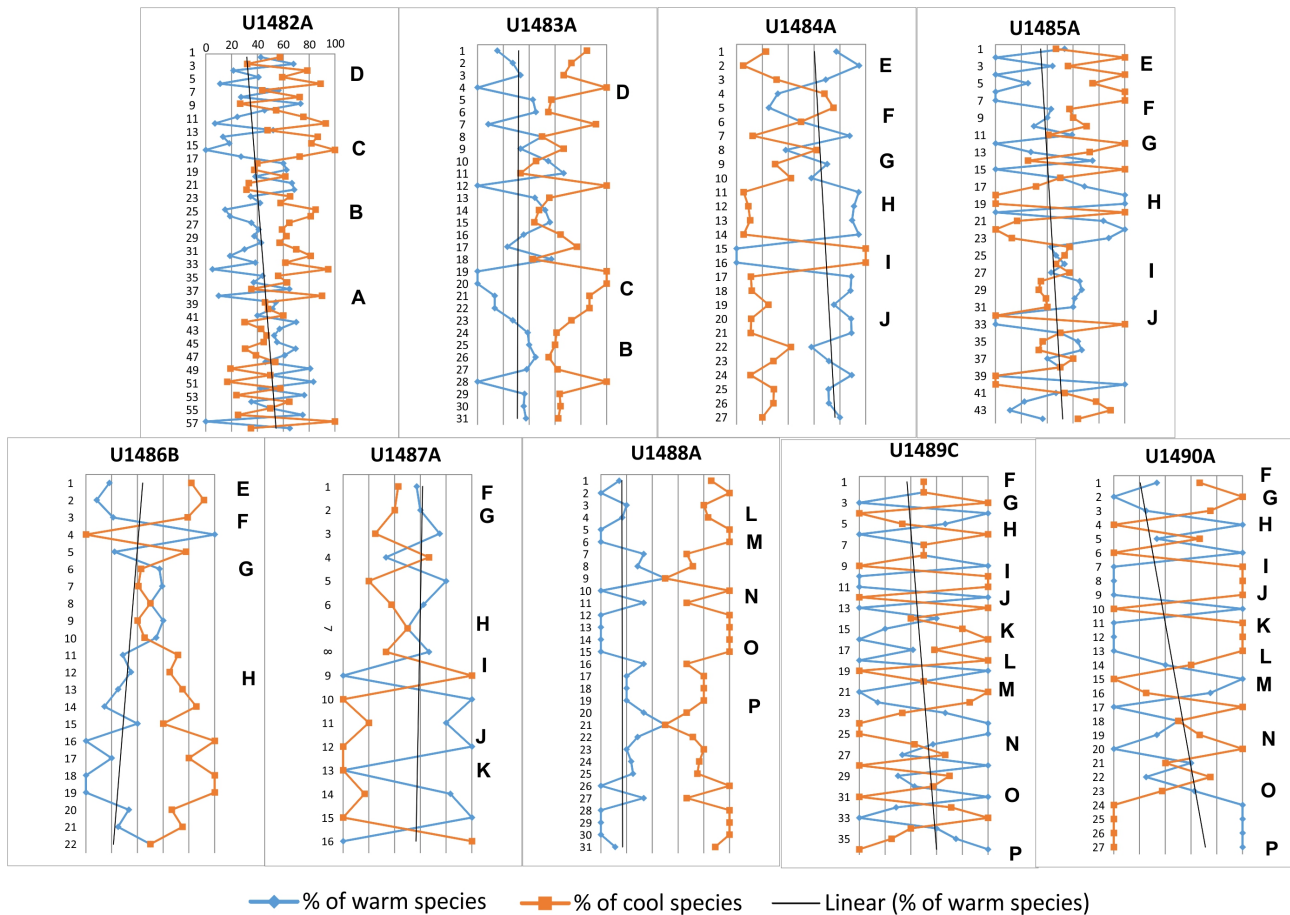


Figure 3 (A - P). Data on spatial abundance (e.g., within each depth transect) of warm and cool species plotted against temporal scale and geological events of sites from Expedition 363 (Stages A to P). Graphs show core catchers samples numbers versus abundance through time.

the spread of grasslands and savannas and a cooler foraminiferal fauna shows it. The Early Pleistocene (=Lower Pleistocene) reaches the time between 2.588 ± 0.005 Ma and 0.781 ± 0.005 Ma (Figure 3C). The base of the Gelasian is designated as the Matuyama (C2r) chronozone (the Gauss-Matuyama magnetostratigraphic boundary, isotopic stage 103). Ice sheets in the Northern Hemisphere started to grow during the Gelasian, in the beginning of the Quaternary glacial stage. The Middle Pleistocene, known as the Ionian stage, from 781 to 126 ka succeeds the Calabrian Stage (the Brunhes-Matuyama reversal) which in turn shows from the beginning of the last interglacial (Marine isotopic stage- MIS 5) to the base of the Holocene (~10.5 ka) and it was verified by the faunal shift from cool to warmer species (Figure 3D).

U1484A

At least two inter glacial and two glacial cycles were recognized on U1484A based on the increase of warm foraminiferal species, and ten major volcanic ash

horizons coinciding with climatic cooling and increase of cool species in this middle-late Pleistocene core. They are therefore representative of cold (glacial) and warm (interglacial) past periods.

The top part of the core in the Late Pleistocene is associated with Tarantian stage, and the age is the end of the Pleistocene epoch or glacial stage (Figure 3E). Sediment is composed of clay rich foraminifer's nanno ooze, and sand, silt and clay. Before that, it is possible to see that the last maximum glacial ends with the cold period, known as the Younger Dryas sub stage which sediment is composed by sand, silt, clay and cool foraminiferal species at 12.900 to 11.700 ka (Figure 3F).

The starting of the stage is the Eemian interglacial phase (Figure 3G) prior to the final glacial episode in the Pleistocene at 126.000 ka (Figure 3H). The Eemian (also called the last interglacial) was the interglacial period, which started around 130.000 ka and ended about 115.000 ka. It corresponds to Marine Isotope Stage 5e and it shows increase of warm foraminiferal species in sediment composed by sand, silt, and clay with periods of clay rich

Foraminifera nanno ooze. Before the Holocene, the last interglacial period has temperatures at at the minimum 2°C warmer, mean sea level of 4-6 m higher than today, with decreases in the Greenland ice sheet. Microfossil and fossil reef proxies indicate mean sea level fluctuations of up to 10 m. This information are important to understand current climate, because mean temperatures around the world during MIS-5e were close to the projected climate change nowadays. The oldest sediments are upper part of middle Pleistocene, in the Ionian stage, reaching a period of geologic time of 0.29 Ma. (Figure 3I). This stage happens after a series of volcanic ash horizons and foraminiferal fauna is colonized by cool species in sand and silt sediments (Figure 3J). It is important to notice that after volcanic ash episodes cool foraminiferal species tend to colonize.

U1485A

Even though U1485A sedimentation rate is twice higher than 1484A, the inter glacial and glacial cycles were similar and based on the increase of warm foraminiferal species, and the seventeen major volcanic ash horizons recorded coincides with climatic cooling and increase of cool species in this middle-late Pleistocene core. The top part of the core in the Late Pleistocene is associated with Tarantian stage, representing the end of the Pleistocene epoch or glacial stage.

In U1486B the Early-Middle Pleistocene transition (c. 1.2-0.5 Ma), or the ‘mid-Pleistocene revolution’, is a vital episode in the history of Earth. Low-amplitude 41-ka obliquity-forced climate cycles of the earlier Pleistocene were substituted in the later Pleistocene by high-amplitude 100-kyr cycles suggestive of ice build-up slowly (increase of global ice volume at 940 ka) with following rapid melting. These climate alterations, especially the increasing severity and duration of cold stages, had a huge consequence on the biota and landscape in the Northern Hemisphere (Figure 3E) The Matuyama-Brunhes palaeomagnetic Chron border (mid-point at 773 ka) is view as Early-Middle Pleistocene Subseries boundary with warm species (Figure 3F). In terms of foraminiferal fauna, there is an inversion of cool-warm-cool species (Figure 3G). Eemian interglacial phase began about 130,000 ka and ended about 115,000 ka, and it corresponds to Marine Isotope Stage 5e, showing increase of warm foraminiferal species in sediment composed by sand, silt, and clay, rich foraminifera and Nano ooze with ash. Figure 3H shows Calabrian, in the Pleistocene, established as ~1.8 Ma—781,000 ka ± 5,000 years supporting cool foraminiferal species. The last magnetic pole reversal (781 ± 5 Ka) is the end of this stage diving into a glacial and drying stage

around the world, which is probably colder and drier than the late Miocene (Messinian) in the Zanclean (early Pliocene) cold period. It has become the second geologic age in the Early Pleistocene.

U1487A

Climate alterations, especially the increasing gravity and duration of cold stages had a profound effect on the microfossils of this site. The same events from U1486 are observed: Figure 3 (E), (F), (G), and (H). Besides that, it is also possible to observe that the bottom of this site exhibits more events such as the Gelasian Stage (Figure 3I), first of four stages of the Pleistocene Series, enclosing deposits during the Gelasian Age (2.588,000 to 1.806,000 ka) of the Pleistocene in the Quaternary Period with warm species (Figure 3J). The Piacenzian is the latest age of the Pliocene, and it reaches the time between 3.6 ± 0.005 Ma and 2.588 ± 0.005 Ma (Figure 3K). Climate of the Piacenzian is wet, moist, and warm period in North America colonized by warm foraminiferal species, occurring after a small chilling period of the Zanclean, which cool species dominating fauna, is similar to sites U1482A and U1483A.

The more recent events from Figure 3F to K are observed at the upper part of the U1488A. This core also shows other events: The Early Pliocene warmth (Figure 3L), at about 4 to 5 Ma, earth had a warm, temperate climate, when the Artic was 8°C warmer than today in a permanent El Nino state and increase of warmer species. The cooling conducted to the setting of temperature patterns of the present, responding to a reduction in atmospheric CO₂ concentration, (100 parts per million) of preindustrial values. The early Pliocene climate had lower austral and zonal temperature gradients but alike maximum ocean temperatures^[23]. During the Zanclean flood (Figure 3M), a hypothetically one to have refilled the Mediterranean Sea at 5.33 Ma, ended the Messinian salinity crisis, and marked the beginning of Zanclean age. Sea-level rise may have reached rates at times greater than 10 m per day. In the Pliocene (5.3 Ma to 2.6 Ma) climate set off drier and cooler, and seasonal, similar to today’s climate. The mean temperature in the mid-Pliocene (3.3 Ma-3.0 Ma) was 2-3 °C elevated than today, sea level rise 25 m, and the Northern Hemisphere ice sheet was short lived prior the beginning of the major glaciation above Greenland during the late Pliocene around 3 Ma. The formation of the Arctic ice cap occurs by an abrupt change in oxygen isotope ratios and ice-rafted cobble in the North Atlantic and Pacific Ocean beds. The global cooling that happened in the Pliocene may have stimulated the disappearance of wet forests and the spread of grasslands

and savannas. The equatorial Pacific Ocean sea surface temperature gradient was lower than the present day, and the sea surface temperature in the East were warmer than nowadays but alike in the west. This condition has been described as a permanent El Niño state. The Alps in Europe halt outward expansion suitable to the increase in erosional flux and as a response to the climatic shift to wetter conditions in Europe during the Mediterranean desiccation at the end of the Miocene (Figure 3N). Zone M13 show Bio horizon base with *Pulleniatina primalis* (6.6 Ma) (Figure 3O). The Tortonian age of the Miocene (11.6-7.25 Ma) present changes in the vegetation compared to modern natural (Figure 3P). Warm and temperate forests covered much of Europe, coastal North America and South-East Asia at this time. Our findings show evidences of the dryness spread in the savanna in central USA, the Middle East and on the Tibetan Plateau. The tropical forests in South America were reduced, however enlarged in the Indian sub-continent and East Africa. Mean annual temperature around the world is probably as much as 4.5 °C higher than today with many sites undergoing higher than modern quantity of precipitation. The foraminiferal assemblages are from intermediate to deep bathyal depths, and both cores U1489B and U1490A show evidence of the same phases (Figures 3F to P) evidenced in U1488A.

5. Discussion

Paleo environmental reconstructions found on down-core variations in the geochemistry of foraminifera depend on the availability of pristine samples. Recrystallization in the sediments tends to homogenize the original geochemical signature affecting, in particular, down-core surface temperature reconstructions [24]. The reconstructions of the deep ocean are less affected by this diagenetic effect because the calcification temperature of benthic foraminifera is closer to the recrystallization temperature in the sediments. However, limiting reconstructions to clay-rich sediments would severely limit the spatial coverage of geochemistry-based reconstructions of surface ocean properties. Thus, other indicators of the state of foraminiferal preservation are important contributor to paleo climatic and paleoceanographic reconstructions. Therefore, if preservation of foraminiferal species is good, these data are accurate tool to understand both natural and geomorphologic evolution and changes. The excellent preservation and the remarkable physical tolerance of the species to higher physical pressure in water and in sediment provided data on at least 11 glacial and interglacial cycles from different cores. These cycles correlated well in all depths from late Oligocene (~24

Mya) to Recent were evidenced by WBF fluctuations recorded by shallower “warm” benthic species (*Bulimina aculeate*, *Laticarinina pauperata*, *Hoeglundina elegans*, *Cibicidoides kullenbergi*, *C. robertsonianus*, *Cibicidoides sp.*) and deeper “cool” species (*Pyrgo murrhina*, *Globobulimina hoeglundi*, *Uvigerina peregrina* *Planulina wuellerstorfi*) (Figures 4, 5, 6 and 7).

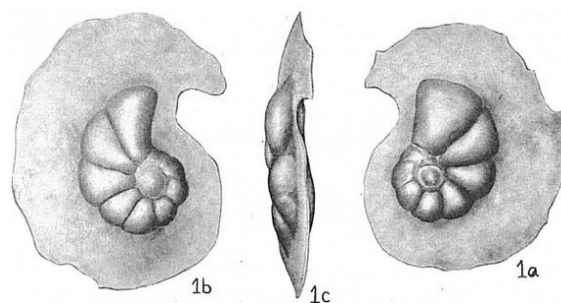


Figure 4. Views of *Laticarinina pauperata*. 1a. Spiral view; 1b. Umbilical view; 1c. Side view (Retired from Cushman, 1931).

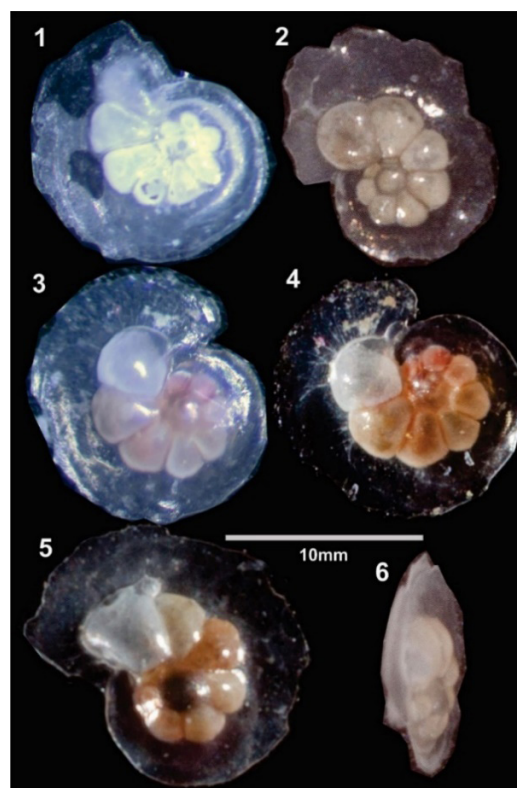


Figure 5. Different views of *Laticarinina pauperata*. 1. Spiral view of a Miocene form of *L. pauperata* found in 23 Mya. 2. Umbilical view of a modern dead specimen found in 1022.77 m depth. 3. Umbilical view of modern living specimen in 1022.77 m. 4. Umbilical view of modern living specimen in 3421 m depth. 5. Spiral view of a modern living specimen in 3421 m depth. 6. Side view of the modern dead specimen found in 3421 m depth.



Figure 6. Deep-water foraminiferal species

1. *Planulina wuellerstorfi* (Schwager, 1866) 363-U1482A-1Hcc; 2. *Ceratobulimina jonesiana* (Brady 1881) 363-U1482A-1Hcc; 3. *Oridorsalis umbonata* (Reuss, 1851) ventral view 363-U1482A-6Hcc; 4. *Oridorsalis umbonata* (Reuss, 1851) 363-U1482A-6Hcc; 5. *Gyroidinoides soldanii* (d'Orbigny 1826) 363-U1482A-7Hcc; 6. *Pleurostomella brevis* (Schwager, 1866) 363-U1482A-7Hcc; 7. *Uvigerina aculeata* (d'Orbigny 1839) 363-U1482A-7Hcc; 8. *Uvigerina auberiana* (d'Orbigny 1839) 363-U1482A-7Hcc; 9. *Rectuvigerina multicostata* (Cushman and Jarvis, 1929) 363-U1482A-15Hcc; 10. *Fissurina lacunata* (Burrows and Holland 1895) 363-U1482A-13Hcc; 11. *Pyrgo lucernula* (Schwager, 1866) 363-U1482A-15Hcc; 12. *Osangularia bengalensis* (Schwager, 1866) 363-U1482A-11Hcc

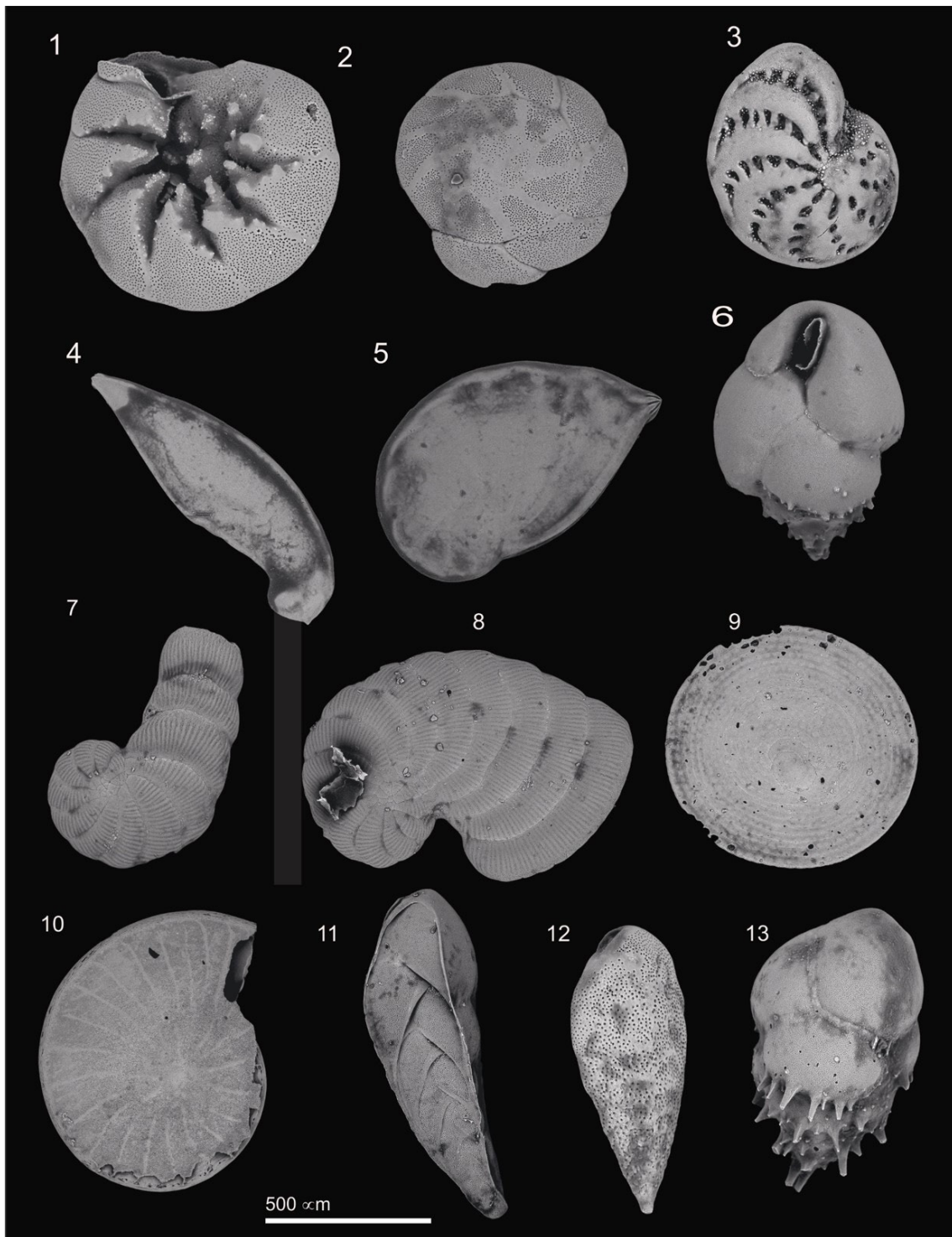


Figure 7. Shallow and reef-dwelling foraminiferal species

1. *Rotalinoides compressiusculus* (Brady 1884) (ventral view) 363-U1484A-15HCC; 2. *Rotalinoides compressiusculus* (dorsal view) 363-U1484A-15HCC; 3. *Elphidium advenum* (Cushman 1922) 363-U1484A-5HCC; 4. *Planularia australis* (Chapman 1915) 363-U1484A-8HCC; 5. *Planularia australis* (Chapman 1915) 363-U1484A-8HCC; 6. *Bulimina marginata* (D'Orbigny 1826) 363-U1484A-11HCC; 7. *Peneroplis planatus* (Fichtel and Moll 1798) 363-U1484A-15HCC; 8. *Coscinospira arietina* (Batsch 1791) 363-U1484A-15HCC; 9. *Amphisorus hemprichii* (Ehrenberg 1839) 363-U1484A-15HCC; 10. *Operculina complanata* (Defrance 1822) 363-U1484A-15HCC; 11. *Bolivinita quadrilatera* (Schwager 1866) 363-U1484A-4HCC; 12. *Bolivina robusta* (Brady 1881) 363-U1484A-4HCC; 13. *Bulimina aculeata* (D'Orbigny 1826) 363-U1484A-3HCC

Sites 1482A and 1483A are in the hydrographic transition that divides the warm tropical water of the Indian-Pacific Western warm pool (IPWP) from the Subtropical water masses. They are located in an area affected by the oceanographic front between cool, nutrient-rich water transfer towards North in the Eastern Indian Ocean by the West Australian Current, and warm, oligotrophic Leeuwin Current waters, resulting in a steep north-south SST gradient. Together, these two sites located along the route of the Indian Through Flow (ITF) as it exits into the Indian Ocean through the Timor Strait between northwestern Australia and Java allow reconstruction of the southwestern extent of the IPWP since early late Miocene. The Timor Strait is one of the main exits of the ITF to the Eastern Indian Ocean ^[25]. Thus, U1482A and U1483A are easily located to facilitate monitoring changes in the intensity and thermal structure of ITF water masses entering the Eastern Indian Ocean ^[26].

In the southern reefal area of Abrolhos (BA, Brazil) ^[27] found *Laticarinina pauperata* in 1.100 m of water depth, and ^[28] used benthic foraminiferal biotas to track changes in the strength and seasonality of the monsoons. During the dry boreal winter monsoon with northeasterly winds, low biological productivity in the Indian Ocean provides low food to deep-sea fauna. As opposed to the intense, wet, southwesterly winds of the southwest (boreal summer) monsoon cause widespread upwelling and high surface productivity ^[29,30], and therefore a high supply of organic particles to the seafloor. This monsoon-linked productivity is large in the Arabian Sea, and in the Bengal Bay, as seen in satellite images collected by the Coastal Zone Color Scanner and SeaWiFS (<http://bluefin.gsfc.nasa.gov/chi/level3.pl>). Deep-sea benthic foraminifera are responsive to total export flux of food to the seafloor and seasonality ^[31-34].

Laticarinina pauperata is from cool, strongly pulsed high seasonality, low to intermediate organic flux sites ^[28]. In according to the Encyclopedia of life, its chronostratigraphic ranges from Mioceno to Recent; its evolution and systematics show first appearance for older bound is at 28.1 Mya (Chattiano Age), and the first appearance for younger bound is 23.03 Mya (Aquitano Age). The last appearance (older bound) is at 3.6 Mya (Piacenziano Age), and the last appearance (younger bound) is at 2.59 Mya (Gelasiano Age). This species lives in all mudlines of the nine cores and it has defined limits of appearances in the past. The environmental ranges for modern habitat are wide for depth (m): 0 - 3100, temperature (°C): -1.260 - 29.191, nitrate (umol/L): 0.038 - 42.384, salinity (PSU): 31.836 - 36.672, oxygen (ml/l): 0.206 - 7.696, phosphate (umol/l): 0.047 - 3.105,

and silicate (umol/l): 1.067 - 125.649 showing species' tolerance.

Among the benthic indicator species studied, *Laticarinina pauperata* ^[35] is unique by its beautiful appearance, cosmopolitan, calcareous epifaunal foraminifera species ^[36] with biconvex trochospiral form being common in bioturbated horizons ^[37]. The presence of these specimens under this huge physical pressure is amazing. Can you imagine 3000 m of water plus 500 m of sediment? Can you imagine the sum of perpendicular force put in to the surface of this species per area? The pressure a liquid applies depends on its depth. This pressure in open conditions is approximated as in "static" or non-moving conditions (even in the moving ocean), because the currents and waves generate only insignificant changes in the pressure. Besides that, foraminiferal tests can suffer taphonomic process known as diagenesis, where sediments are compacted and buried under layers of sediment and stick to minerals that precipitate.

Here we show that preserved foraminifera were able to contribute to paleoceanographic reconstructions of at least 11 glacial and interglacial cycles correlated with depths from late Oligocene to Recent showing that foraminiferal fluctuations track tropical and subtropical fronts, in the Miocene, and that besides the delicate *Laticarinina pauperata* morphology it has great tolerance to physical pressure and is a remarkable paleo indicator.

6. Conclusions

Excellent preserved microfossils with scarce evidence of mineral overgrowth, recrystallization and abraded shells, show that the sedimentological setting with varying amounts of facies and foraminiferal forms from different paleo depth are very suitable for this research. Sites composed of nannofossil ooze with different amounts of siliceous microfossils (diatoms and radiolarians), and clay ranging from the Miocene to Recent day, are dominated by foraminifers calcareous species and less than 5% of the assemblages is composed by agglutinated forms. A mixed fauna shows alterations in the middle Pleistocene to Recent present terrigenous and hemi pelagic sediment with well-preserved calcareous nannofossils, benthic and planktonic foraminifers which unravels habitat transition in down core catchers' samples. The habitat change observed downhole show that deeper water benthic foraminifers inhabits upper and lower parts of the core; while middle part of the core consists of a mix of deep and shallow water benthic foraminifers, including reef-dwelling species in a 1000 m deep, including *Operculina complanata*, *Amphisorus hemprichii*, *Coscinospira arietina*, and *Peneroplis planatus*. These species are

characteristic of water depths shallower than 45 m, and probably were carried to this site with other debris.

The presence of deep-water and cool forms without any large contribution from shallower water or reef faunas in a high abundant volcanic ash environment is also a new finding. Our low-resolution study of the relation of WBF shows that with the exception of core 1486B, all of them show that older sediments indicate warmer periods than today, a tendency of what is expected from Miocene to Recent.

The excellent preservation and the remarkable physical tolerance that species present to higher physical pressure from water column and sediment provided data on at least 11 glacial and interglacial cycles from different cores. These cycles correlated well in all depths with occurrence from late Oligocene (~24 million years ago) to Recent were evidenced by WBF fluctuations recorded by the shallower warm benthic species (*Cibicidoides* sp., *Laticarinina pauperata*, *Cibicidoides kullenbergi*, *C. robertsonianus*, *Bulimina aculeata*, *Hoeglundina elegans*) and deep-water cool species (*Uvigerina peregrina*, *Pyrgo murrhina*, *Globobulimina hoeglundi*, *Planulina wuellerstorfi*). *Laticarinina pauperata* is unique by its beautiful and delicate appearance, but it is also an excellent calcareous epifaunal foraminifer from strongly pulsed, high seasonality, cool, low to intermediate organic flux, ranging from Miocene to Recent. It is also living these days in all mudlines of the nine cores that we collected and we show that this form is common in bioturbated horizons and tolerant to high physical pressure. In addition, taphonomic process known as diagenesis can prevent the studies by destroying the tests through time, and our findings were able to unravel many interesting information because of the tolerance and preservation of the shells.

Acknowledgements

This article used samples collected by the Ocean Drilling Program (ODP) and provided by the International Ocean Discovery Program (IODP), sponsored by the U.S. National Science Foundation (NSF) and participating countries. We are thankful for the Project Geohazards and Tectonics (CAPES Grant 88887.091714/2014-01, IODP Program). Research was also supported by IODP/CAPES Brazil fellowship granted to PE to go aboard the Research Vessel Joides Resolution in 2016. This research would not have been conducted without funding from Ciências do Mar II (CAPES Coordenação de Aperfeiçoamento de Pessoal de Nível Superior) through the Project Processos oceanográficos na quebra da plataforma continental do nordeste brasileiro: fundamentos científicos para o planejamento espacial

marinho (n°43/2013, 23038.004320/2014-11) through for the Post-Doc Fellowship for Eichler at the Moss Landing Marine Laboratories of the San Jose State University (MLML/SJSU), and at the Ocean Sciences Department of the University of California at Santa Cruz (UCSC) (grants N°88887.305531/2018-00, N°88881.188496/2018-01). We are also grateful for the International Ocean Discovery Program (IODP) in the Texas A&M University (USA) (Grant N°9999.000098/2017-05) and to the Technical Support to Strengthen National Palaeontology (Apoio Técnico para Fortalecimento da Paleontologia Nacional, Ministério da Ciência e Tecnologia MCTI/National Research Council CNPq N° 23/2011, N° 552976/2011-3) for funding opportunity. We are grateful for the EcoLogicProject for the manuscript detailed editing.

References

- [1] Debenay, J.P., Geslin, E., Eichler, B.B., Duleba, W., Sylvestre, F. and Eichler, P., (2001). Foraminiferal assemblages in a hypersaline lagoon, Araruama (RJ) Brazil. *The Journal of Foraminiferal Research*, 31(2), pp.133-151.
- [2] Hallock, P., 1984. Distribution of selected species of living algal symbiont-bearing foraminifera on two Pacific coral reefs. *The Journal of Foraminiferal Research*, 14(4), pp.250-261.
- [3] Hallock, P., 2000. Larger foraminifera as indicators of coral-reef vitality. In *Environmental micropaleontology* (pp. 121-150). Springer, Boston, MA.
- [4] A'ziz, A.N.A., Minhat, F.I., Pan, H.J., Shaari, H., Saelan, W.N.W., Azmi, N., Manaf, O.A.R.A. and Ismail, M.N., 2021. Reef foraminifera as bioindicators of coral reef health in southern South China Sea. *Scientific Reports*, 11(1), pp.1-13.
- [5] Murray, J. 2006. *Ecology and Applications of Benthic Foraminifera*. xi + 426 pp. Cambridge, New York, Melbourne: Cambridge University Press.
- [6] Allen, S. 2010. Environmental controls and distributions of surface foraminifera from the Otter estuary salt marsh, UK: their potential use as sea level indicators. *Plymouth Student Scientist* 4, 293-324.
- [7] Eichler, P.P.B., Eichler, B.B., de Miranda, L.B. and Rodrigues, A.R., 2007. Modern foraminiferal facies in a subtropical estuarine channel, Bertioga, São Paulo, Brazil. *The Journal of Foraminiferal Research*, 37(3), pp.234-247.
- [8] Eichler, P.P., Billups, K. and Cardona, C.C.V., 2010. Investigating faunal and geochemical methods for tracing salinity in an Atlantic coastal lagoon, Delaware, USA. *The Journal of Foraminiferal Research*, 40(1), pp.16-35.

- [9] Horton, B.P. and Murray, J.W., 2007. The roles of elevation and salinity as primary controls on living foraminiferal distributions: Cowpen Marsh, Tees Estuary, UK. *Marine Micropaleontology*, 63(3-4), pp.169-186.
- [10] Eichler, P.P., Billups, K., Vital, H. and De Moraes, J.A., 2014. Tracing thermohaline properties and productivity of shelf-water masses using the stable isotopic composition of benthic foraminifera. *The Journal of Foraminiferal Research*, 44(4), pp.352-364.
- [11] Martins, M.V.A., Moreno, J.C., Miller, P.I., Miranda, P., Laut, L., Pinheiro, A.E.P., Yamashita, C., Terroso, D.L., Rocha, F., Bernardes, C., 2017. Biocenoses of benthic foraminifera of the Aveiro Continental Shelf (Portugal): influence of the upwelling events and other shelf processes. *Journal of Sedimentary Environments*, 2 (1): 9-34.
- [12] Carson, B. E., Francis, J. M., R. M. Leckie, A. W. Droxler, G. R. Dickens, S. J. Jorry, S. J. Bentley, L. C. Peterson, and B. N. Opdyke, 2008. Benthic foraminiferal response to sea level change in the mixed siliciclastic-carbonate system of southern Ashmore Trough (Gulf of Papua), *J. Geophys. Res.*, 113, F01S20.
DOI: 10.1029/2006JF000629.
- [13] Lutze, G. F., 1977. Neogene benthonic foraminifera from Site 369, Leg 41. In Lancelot, Y., Seibold, E., et al., Initial Reports of the Deep Sea Drilling Project, v. 41: Washing-ton (U.S. Government Printing Office), p. 659-666.
- [14] Lutze, G.F. 2007. Benthic Foraminifers at Site 397: Faunal Fluctuations and Ranges in the Quaternary. doi:10.2973/dsdp.proc.47-1.111.1979DSDP Volume XLVII Part 1.
- [15] Fedorov A.V., Philander, S.G. 2000. Is El Nino Changing? *Science*, 288: 1997-2002. Rasmusson, E.M., and Arkin, P.A., 1993. A global view of large-scale precipitation variability. *Journal of Climate*, 6(8):1495-1522.
- [16] Pierrehumbert, 2000. Climate change and the tropical Pacific: the sleeping dragon wakes, *Proc. Natl. Acad. Sci. U.S.A.*, 97(4): 1355-1358.
- [17] Rasmusson, E.M., and Arkin, P.A., 1993. A global view of large-scale precipitation variability. *Journal of Climate*, 6(8):1495-1522.
- [18] Billups, K. Eichler, P. P. B., Vital H. 2020. Sensitivity of Benthic Foraminifera to Carbon Flux in the Western Tropical Pacific Ocean. *Journal of Foraminiferal Research*; 50 (2): 235-247.
DOI: <https://doi.org/10.2113/gsjfr.50.2.235>.
- [19] Rosenthal, Y., Holbourn, A., Kulhanek, D.K., and the Expedition 363 Scientists, 2017. Expedition 363 Preliminary Report: Western Pacific Warm Pool. International Ocean Discovery Program. <http://dx.doi.org/10.14379/iodp.pr.363.2017>.
- [20] Morkhoven, F.P.C.M. Van, Berggren, W.A. and Edwards, A.S. 1986. Cenozoic cosmopolitan deep-water benthic foraminifera, *Bulletin des Centres de Recherches Exploration-Production Elf-Aquitaine. Mémoire.*, v.11, p.421.
- [21] Holbourn, A., Kuhnt, W., Schulz, M. and Erlenkeuser, H., 2005. Impacts of orbital forcing and atmospheric carbon dioxide on Miocene ice-sheet expansion. *Nature*, 438(7067), pp.483-487.
- [22] Jones, R.W. 1994. *The Challenger Foraminifera*. Oxford University. Press, Oxford, ix+149pp.
- [23] Fedorov, A.V., Brierley, C.M., Lawrence, K.T., Liu, Z., Dekens, P.S., Ravelo, A.C. 2013. Patterns and mechanisms of early Pliocene warmth. *Nature*: 496(7443): 43-49.
DOI: 10.1038/nature12003.
- [24] Pearson, P.N., Ditchfield, P.W., Singano, J. and Harcourt-Brown, K.G., 2001. Warm tropical sea surface temperatures in the Late Cretaceous and Eocene epochs. *Nature*, 413(6855), p.481.
- [25] Vranes, K. and Gordon, A.L., 2005. Comparison of Indonesian throughflow transport observations, Makassar Strait to eastern Indian Ocean. *Geophysical Research Letters*, 32(10).
- [26] Xu, J., Holbourn, A., Kuhnt, W., Jian, Z. and Kawamura, H., 2008. Changes in the thermocline structure of the Indonesian outflow during Terminations I and II. *Earth and Planetary Science Letters*, 273(1-2), pp.152-162.
- [27] Oliveira-Silva, P., Barbosa, C. F. and Soares-Gomes, A. "Distribution of macrobenthic foraminifera on Brazilian Continental margin between 18°S-23°S." *Revista Brasileira de Geociências* 35.2 (2016): 209-216.
- [28] Gupta, A. K., and Thomas, E. 2003. Initiation of Northern Hemisphere glaciation and strengthening of the northeast Indian monsoon: Ocean Drilling Program Site 758, eastern equatorial Indian Ocean. *Geology* 31.1 (): 47-50.
- [29] Banse, K. and English, D.C., 1994. Seasonality of coastal zone color scanner phytoplankton pigment in the offshore oceans. *Journal of Geophysical Research: Oceans*, 99(C4), pp.7323-7345.
- [30] Gregg, W.W. and Conkright, M.E., 2002. Decadal changes in global ocean chlorophyll. *Geophysical Research Letters*, 29(15), pp.20-1.
- [31] Murray, J.W. and Smart, C.W., 1994. Distribution of

- smaller benthic foraminifera in the Chagos Archipelago, Indian Ocean. *Journal of micropalaeontology*, 13(1), pp.47-53.
- [32] Jannink, N.T., Zachariasse, W.J. and Van der Zwaan, G.J., 1998. Living (Rose Bengal stained) benthic foraminifera from the Pakistan continental margin (northern Arabian Sea). *Deep Sea Research Part I: Oceanographic Research Papers*, 45(9), pp.1483-1513.
- [33] Loubere, P. and Fariduddin, M., 1999. Benthic foraminifera and the flux of organic carbon to the seabed. In *Modern foraminifera* (pp. 181-199). Springer, Dordrecht.
- [34] Ohkushi, K.I., Nemoto, N., Murayama, M., Nakamura, T. and Tsukawaki, S., 2000. Paleooceanography of the Oyashio Area during the Last 20, 000 Years Based on Benthic Foraminifera. *The Quaternary Research (Daiyonki-kenkyu)*, 39(5), pp.427-438.
- [35] Parker, K.W. and Jones, R.T., 1865. VI. On some foraminifera from the North Atlantic and Arctic Oceans, including Davis Straits and Baffin's Bay. *Philosophical transactions of the Royal Society of London*, (155), pp.325-441.
- [36] Corliss, B.H. and Chen, C., 1988. Morphotype patterns of Norwegian Sea deep-sea benthic foraminifera and ecological implications. *Geology*, 16(8), pp.716-719.
- [37] King, S.C., Kemp, A.E., Murray, J.W., 1995. Benthic foraminifer assemblages in Neogene laminated diatom ooze deposits in the eastern equatorial Pacific Ocean (Site 844). In: Mayer, L.A., Pisias, N.G., Jancsek, T.R., Palmer-Julson, A., van Andel, T.H. (Eds.), *Proc. Ocean Drill. Prog. Sci. Results vol. 138*, 665 - 673.